MODELLING AND NUMERICAL SIMULATION OF HYDROGEN JET FIRES FOR INDUSTRIAL SAFETY ANALYSES – COMPARISON WITH LARGE-SCALE EXPERIMENTS

Rian, K.E.[1]
[1] **DNV GL, P.O. Box 1260 Sluppen, NO-7462 Trondheim, Norway,**
Kjell.Erik.Rian@dnvgl.com

ABSTRACT

Reliable predictive tools for hydrogen safety engineering are needed to meet increased and more widespread use of hydrogen in the society. Industrial models and methods used to establish thermal radiation hazard safety distances from hydrogen jet fires are often based on models previously developed for hydrocarbon jet fires. Their capability of predicting radiative heat fluxes from hydrogen jet fires has often only been validated against small-scale or medium-scale jet flame experiments. However, large-scale hydrogen jet fire experiments have shown that thermal radiation levels can be significantly higher than one might expect from extrapolation of experience on smaller hydrogen flames. Here, two large-scale horizontal hydrogen jet fires (from a 20.9 mm and a 52.5 mm diameter release, respectively) have been modelled and simulated with the advanced industrial CFD code KAMELEON FIREEX KFX® based on the Eddy Dissipation Concept by Magnussen for turbulent combustion modelling. The modelling of the high-pressure hydrogen gas releases is based on a pseudo-source concept using real-gas thermodynamic data for hydrogen. The discrete transport method of Lockwood and Shah is used to calculate the radiative heat transfer, and radiative properties of water vapour are modelled according to Leckner. The predicted thermal radiation is compared to data from large-scale hydrogen jet fire experiments and discussed. This work was conducted as part of a KFX-H2 R&D project supported by the Research Council of Norway.

1.0 INTRODUCTION

Hydrogen will be an important energy carrier in an environmentally friendly and sustainable society. Safe storage and handling of large quantities of hydrogen is a challenge. Reliable predictive tools for hydrogen safety analyses are therefore essential for planning and operation of hydrogen facilities and infrastructure. Industrial models and methods used to establish thermal radiation hazard safety distances from hydrogen jet fires are often based on simplified, empirical models previously developed for hydrocarbon jet fires, see e.g. [1, 2]. Moreover, their capability of predicting radiative heat fluxes from hydrogen jet fires has often only been validated against small-scale or medium-scale jet flame experiments, see e.g. [3-5]. Large-scale hydrogen jet fire experiments have shown that thermal radiation levels can be significantly higher than one might expect from extrapolation of model results based on smaller hydrogen flames [6]. In addition, jet fires in realistic environments are often significantly affected by various geometries, ventilation and atmospheric conditions. Simpler prediction models are normally developed for unobstructed, idealised free jet flames and will typically not be able to account properly for effects of more complex conditions involved in realistic jet fire scenarios. Today, predictive tools based on Computational Fluid Dynamics (CFD) have proven very useful for quantitative consequence analyses of fire hazards in realistic environments [7].

KAMELEON FIREEX KFX® is an industrial CFD simulator for detailed three-dimensional transient predictions of gas dispersion, fires and explosions under realistic conditions. The KFX™ simulation technology has been developed over several decades by ComputIT, NTNU and SINTEF in Norway in close collaboration with major international oil and gas companies, research laboratories, engineering and risk management companies and the Research Council of Norway. Today, the KFX™ development is continued by DNV GL. KFX™ is originally made for consequence predictions of hydrocarbon related hazards in the oil and gas industries. The present work is a part of a recent KFX™ R&D project on hydrogen modelling supported by the Research Council of Norway (BIA project No. 261752). The KFX™ modelling of hydrogen jet fires based on Magnussen's Eddy Dissipation

Concept is described below, including brief descriptions of the high-pressure hydrogen gas release modelling and thermal radiation modelling. Further, thermal radiation predictions from KFX™ simulations are compared to data from two large-scale hydrogen jet fire experiments performed at the Spadeadam test site in the UK [6] and discussed.

2.0 COMBUSTION MODELLING BY THE EDDY DISSIPATION CONCEPT

The physics of fires is similar to what we find in any turbulent combustion environment, even though the overall timescale and boundary conditions or the properties of the flammable gas may be very different. In a turbulent reacting flow, the chemical reactions take place in the fine structures of the turbulent fluid, i.e. in sheets or vortices whose smallest linear dimension is substantially smaller than one millimetre and where the rate of combustion is largely dominated by the exchange rate between the reacting structures and the surrounding fluid. These fine structure regions are localised in the highly strained regions between the bigger eddies. In KFX™ the Eddy Dissipation Concept (EDC) by Magnussen is the basis for the treatment of the complex interaction between the chemical reactions and the turbulent flow [8]. The modelling of this interaction is essential in modelling of fire evolution and fire mitigation where physical processes such as ignition, combustion evolution, flame propagation, extinction, flame stability and thermal radiation need to be considered.

In the EDC, a turbulence cascade model [9] connects the fine structure behaviour to the larger scale characteristics of turbulence like the turbulence kinetic energy, k (m^2/s^2), and its dissipation rate, ε (m^2/s^3). The following characteristic scales for the fine structures can be obtained [8]:

$$u^* = 1.75(\varepsilon \cdot \nu)^{1/4} \text{ and } L^* = 1.43\nu^{3/4}/\varepsilon^{1/4}, \quad (1)$$

where u^* is the fine structure characteristic velocity (m/s), L^* is the fine structure characteristic length scale (m), ε is the rate of dissipation of turbulence kinetic energy (m^2/s^3), and ν is the kinematic viscosity (m^2/s). The characteristic scales for the fine structures are closely related to the Kolmogorov scales. Further, chemical reactions take place when reactants are mixed at a molecular level at sufficiently high temperature and have enough time to react. It is known that the microscale processes which are decisive for the molecular mixing as well as dissipation of turbulence energy into heat are severely intermittent, i.e. concentrated in isolated regions whose entire volume is only a small fraction of the volume of the fluid. An important assumption in the EDC is that most of the reactions occur in the fine structures of these regions. The mass fraction occupied by the fine structures, γ^*, can be formulated as

$$\gamma^* = (u^*/u')^2 \quad \text{or expressed by } k \text{ and } \varepsilon \text{ as} \quad \gamma^* = 4.6 \cdot (\nu \cdot \varepsilon/k^2)^{1/2} \quad (2)$$

Here, u' is a characteristic velocity scale for the larger, most energy containing eddies. The dissipation of turbulence energy and the molecular mixing is fast in the fine structures. Hence, the fine structures can be treated conceptually as well-stirred chemical reactors. The transfer of mass per unit of fluid and unit of time, $\dot{m}$ (s^{-1}), between the fine structures and the surrounding fluid can be expressed as

$$\dot{m} = 2 \cdot u^*/L^* \cdot \gamma^* \text{ or } \dot{m} = 11.2 \cdot \varepsilon/k \quad (3)$$

Further, the mean rate of reaction, $\bar{R}_i$ ($kg/m^3/s$), for species i can be expressed as

$$-\overline{R}_i = \frac{\bar{\rho}\dot{m}\chi}{1-\gamma^*\chi}(\tilde{Y}_i - Y_i^*), \quad (4)$$

where $\bar{\rho}$ is the mean fluid density (kg/m^3), ρ^* is the fine structure fluid density (kg/m^3), χ is the reacting fraction of the fine structures, $\tilde{Y}_i$ is the mean mass fraction of species i, and Y_i^* is the fine structure mass fraction of species i. The EDC can be used with full detailed chemical kinetics for both turbulent premixed and diffusion flames. However, the fast chemistry limit treatment of chemical reactions will typically be sufficient for most fire simulations of practical interest. When fast

chemistry is assumed, the state in the fine structure regions is taken as equilibrium, or at a prescribed state. If one of the major components, fuel or oxidant, is assumed to be completely consumed in the fine structure reactor, the mean rate of reaction of fuel, $\bar{R}_{\mathrm{fu}}$, can be formulated as

$$-\bar{R}_{\mathrm{fu}} = \frac{\bar{\rho}\dot{m}\chi}{1-\gamma^{*}\chi} \cdot \tilde{Y}_{\mathrm{min}} \tag{5}$$

where $\tilde{Y}_{\mathrm{min}}=\min\left[\tilde{Y}_{\mathrm{fu}}, \frac{1}{r}\tilde{Y}_{\mathrm{ox}}\right]$, i.e. the reaction rate is limited by which of the reactants, fuel or oxidant, that is in short supply.

Furthermore, the fraction of the fine structures that is sufficiently heated to react can be expressed as

$$\chi = \frac{\tilde{Y}_{\mathrm{pr}}/(1+r)}{\tilde{Y}_{\mathrm{min}}+\tilde{Y}_{\mathrm{pr}}/(1+r)}, \tag{6}$$

where r denotes the stoichiometric oxidant requirement. $\tilde{Y}_{\mathrm{fu}}$, $\tilde{Y}_{\mathrm{ox}}$ and $\tilde{Y}_{\mathrm{pr}}$ are the local mean mass fractions of fuel, oxidant and reaction products, respectively. Further details on the EDC and the theoretical reasoning behind the concept are given by Magnussen [8].

3.0 KFX™ MODELLING AND COMPUTATIONAL ELEMENTS

KFX™ is a finite-volume CFD code which solves the fundamental conservation equations for three-dimensional, time-dependent turbulent flow and combustion using a non-uniform Cartesian grid. KFX™ includes powerful CAD import capabilities where CAD geometries, including electronic maps of terrain, buildings, modules, process plants, etc., are converted automatically into a computational grid including cells for solid constructions or surface/volume porosities used by the KFX™ calculation model.

Turbulence is modelled with the standard *k-ε* model including buoyancy terms and standard constants. A feature of the EDC combustion model implemented in KFX™ is that turbulent flame propagation is automatically generated by the model and not specified by an empirical expression for the turbulent burning velocity. Extinction can be modelled based on chemical time scales obtained from detailed chemistry calculations.

Thermal radiation is modelled according to the discrete transport method of Lockwood and Shah [10]. In hydrogen-air flames, the only significant source of radiative emission is excited-state H_2O^* molecules. In KFX™, the absorption coefficient for water vapour is modelled according to Leckner [11].

A pseudo-source concept for high-pressure hydrogen gas releases is used to model the expansion process at subgrid level to obtain equivalent expanded flow characteristics at atmospheric conditions. The release source model is developed from fundamental physical principles of conservation of mass, momentum and energy for a control volume, and homogeneous equilibrium conditions are assumed during the expansion process [12, 13]. The expansion is modelled as an isentropic process from stagnation conditions to the orifice conditions followed by a constant total enthalpy process for the further expansion to atmospheric conditions. The modelling is based on real-gas thermodynamic data from an accurate fundamental equation of state for hydrogen [14,15].

Wind boundary conditions are modelled by logarithmic wind profiles for wind velocity, turbulence energy and rate of dissipation of turbulence energy based on a prescribed wind velocity at a given reference height, a Monin-Obukhov length scale, a roughness scaling height, the current latitude for calculation of Coriolis effects and the wind temperature. The Monin-Obukhov length scale can be estimated based on the Pasquill class for atmospheric stability [16].

KFX™ includes several other models and features that were not relevant for the hydrogen jet fire simulations performed in this work, such as a soot formation and combustion model, multicomponent pool spreading models and a Lagrangian spray model for liquid releases of hydrocarbons or water. This enables, for example, modelling of water-based fire mitigation systems such as deluge, monitors and sprinklers. Furthermore, KFX™ is interfaced with the finite element structure response code USFOS for non-linear dynamic structural response analysis.

4.0 DESCRIPTION OF THE LARGE-SCALE HYDROGEN JET FIRE EXPERIMENTS

In 2008, two large-scale hydrogen jet fire experiments were conducted at the former Advantica Spadeadam Test Site (today DNV GL's Spadeadam Test Site) in North Cumbria, UK, on behalf of Air Products and Chemicals Inc. [6]. In the experiments compressed hydrogen gas at a nominal pressure of 60 barg was released horizontally, 3.25 m above the ground. For Jet Fire No. 1 hydrogen was released through a pipe bore size of 20.9 mm, and for Jet Fire No. 2 a pipe bore size of 52.5 mm was applied. Mass flow rates of 1.0 kg/s and 7.5 kg/s, respectively, were calculated using orifice plate measurements of pressure and temperature. Special care was taken to ensure that no particles were entrained into the flame, either from the internal piping or from the ground below. Before the tests were conducted, the gas storage and delivery system were purged several times to clear them for contaminants. In addition, a concrete pad with steel sheeting was used under and downstream the release location to prevent the entrainment of dirt particles from the ground, see Fig. 1.

Figure 1. Release setup for the large-scale hydrogen jet fire experiments at the Spadeadam test site (Photo from Ekoto et al. [6]).

Boundary and ambient conditions for the two hydrogen jet fire experiments are summarized in Table 1. The wind speed and wind direction, as well as the ambient temperature and relative humidity, were measured at a weather tower located approximately 111 m upstream from the release point. The given values for the wind speed in Table 1 have been calculated for the wind speed 10 m above the ground at the release point. Furthermore, the jet release was orientated 67° relative to true north, and the wind directions given in Table 1 are also relative to true north. That is, the mean wind direction for Jet Fire No. 1 was towards the jet release at an angle of 1.5°, and the mean wind direction for Jet Fire No. 2 was towards the jet release at an angle of 28.3°.

Table 1. Boundary and ambient conditions for the hydrogen jet releases.

Jet No.	D_i (mm)	$\dot{m}$ (kg/s)	P_0 (barg)	T_0 (K)	RH (%)	T_{amb} (K)	P_{amb} (mbar)	U_{wind} (m/s)	ϕ_{wind} (°)
1	20.9	1.0	62.1	308.7	94.3	280	1022	3.4	68.5
2	52.5	7.5	61.4	287.1	94.2	287	1011	2.6	38.7

Wide-angle (150° field of view) radiometers mounted on tripods were used to measure incident

radiation at 13 locations, see Fig. 2. Detailed information on the position for each radiometer is given in Table 2. Note that the radiometer positions are given relative to the release point (0, 0, 0), and that the vertical position (above the ground) is represented by the y-axis for the reported experiments.

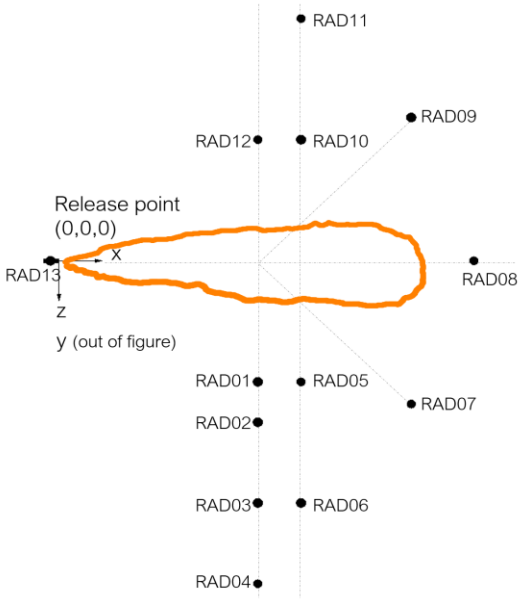

Figure 2. Schematic of the radiometer layout during the hydrogen jet fire experiments.

Table 2. Radiometer positions relative to the release point (0,0,0) for the jet fire experiments.

	Jet Fire No. 1			Jet Fire No. 2		
Radio-meter	x (m)	y (m)	z (m)	x (m)	y (m)	z (m)
RAD01	11.0	-2.4	7.5	23.0	-2.4	15.0
RAD02	11.0	-1.7	12.5	23.0	-1.7	20.0
RAD03	11.0	-1.9	15.0	23.0	-1.9	30.0
RAD04	11.0	-0.3	17.5	23.0	-0.3	40.0
RAD05	16.0	-2.4	7.5	28.0	-2.4	15.0
RAD06	16.0	-1.8	12.5	28.0	-1.8	30.0
RAD07	21.6	-1.8	10.6	40.7	-1.8	17.7
RAD08	26.0	-1.5	0.0	48.0	-1.5	0.0
RAD09	21.6	-1.2	-10.6	40.7	-1.2	-17.7
RAD10	16.0	-1.3	-7.5	28.0	-1.3	-15.0
RAD11	16.0	-0.5	-12.5	28.0	-0.5	-30.0
RAD12	11.0	-1.8	-7.5	23.0	-1.8	-15.0
RAD13	-1.0	-1.0	0.0	-1.0	-1.0	0.0

Four radiometers (RAD01, RAD02, RAD03 and RAD04) were positioned perpendicular to the release axis and a pre-estimated flame centre at different locations in the positive z-direction. To check for flame symmetry, a radiometer (RAD12) was positioned on the opposite side. Four radiometers (RAD05, RAD06, RAD10 and RAD11) were positioned 5 m downstream from the pre-estimated flame centre, with two radiometers on each side of the release axis. All these radiometers were orientated normal to the release axis. Two radiometers (RAD07 and RAD09) were positioned far downstream the release point and orientated at an angle of 45° relative to the release axis. One radiometer (RAD08) was positioned directly downstream of the flame and orientated along the release

axis. The last radiometer (RAD13) was positioned upstream of the flame and orientated along the release axis.

Flame ignition was remotely initiated by an incendiary device positioned close to the release pipe. Measurements were done for discrete averaging time periods to ensure that representative mean values were obtained. For Jet Fire No. 1 the averaging period was between 50 and 90 seconds after spark ignition, during which a steady stagnation pressure was maintained. For the relatively large diameter release for Jet Fire No. 2, it was not possible to maintain a steady stagnation pressure due to limited hydrogen storage capacity and high flow rates. However, a quasi-steady stagnation pressure could be assumed for an averaging period between 10 and 20 seconds after ignition when the decay in the stagnation pressure was sufficiently slow.

Further details on the experimental setup and measurements are given by Ekoto et al. [6].

5.0 NUMERICAL SIMULATION SETUP

The two hydrogen jet fire experiments were modelled in KFX™ using one jet release cell in an open computational domain with a solid boundary for the ground and open wind boundaries for all the other boundaries of the computational domain. Very limited information was found on the geometrical structures upstream from the release point (cf. [6]), and these geometries were therefore not included in the simulation setup. For the high-pressure hydrogen gas release, equivalent release conditions at atmospheric pressure were calculated using a pseudo-source concept [12, 13] and accurate real-gas thermodynamic data [14, 15]. Input data for the release modelling are found in Table 1 above. KFX™ logarithmic wind inlet profiles were used for the simulations, and the atmospheric stability conditions were assumed to be neutral, i.e. Pasquill stability class D [16].

For Jet Fire No. 1, a computational domain of 70 m × 60 m × 45 m was defined, and the computational domain consisted of 943312 computational cells. The smallest characteristic cell size length of the non-uniform jet grid was ~0.053 m. For Jet Fire No. 2, a computational domain of 110 m × 100 m × 80 m was defined, and the computational domain consisted of 1105520 computational cells. The corresponding smallest characteristic cell size length of the non-uniform jet grid was ~0.151 m.

6.0 RESULTS AND DISCUSSION

Figure 3 shows predicted iso-contours of projected maximum gas temperature for Jet Fire No. 1.

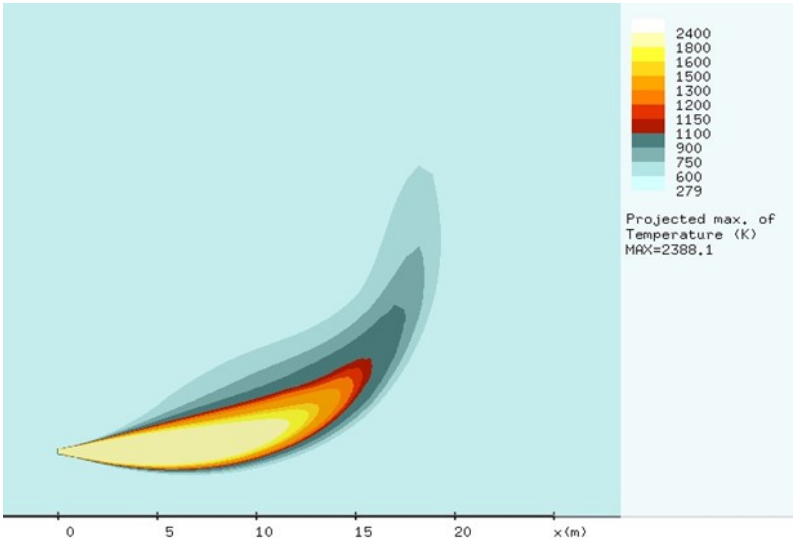

Figure 3. Predicted iso-contours of projected maximum gas temperature for Jet Fire No. 1.

This plot may give a qualitative impression of the predicted flame. In the experiment, it was noticed that the flame was quite luminous, and the flame length was reported to be 17.4 m [6]. The predicted jet flame length may seem to be a little underpredicted compared to the estimated flame length from the experiments. Figure 4 shows a detailed comparison of the predicted incident thermal radiation to the measured incident thermal radiation at the thirteen radiometer locations. Simulation results for atmospheric conditions with dry air are also included in Fig. 4 for comparison. As expected, the predicted incident thermal radiation is a little higher for atmospheric conditions with dry air than for atmospheric conditions with humid air. The overall agreement between the predicted and measured incident thermal radiation is very good. Some deviations between predictions and measurements are observed for radiometer No. 10 and radiometer No.13 for this jet fire. Radiometer No. 10 is positioned symmetric to radiometer No. 5 in the experiments (and in the simulation). The mean wind direction during the jet fire test is also almost parallel and straight against the release direction. The measured incident thermal radiation for radiometer No. 10 is therefore expected to be closer to the measured incident thermal radiation for radiometer No. 5, as predicted by KFX™. The positioning of radiometer No. 13 can be discussed, as it was installed 1 m behind (upstream) the end of the release pipe and 1 m below the release axis. Because of the proximity to the release point, it is possible that the visible flame could extend beyond the view area of the radiometer and therefore lead to lower measured incident radiation for this sensor. However, this was deemed unlikely by the experimentalists [6]. Furthermore, the jet release was modelled in KFX™ as a jet release cell without geometries upstream the release point. It is therefore possible that a lower measured incident thermal radiation for radiometer No. 13 could result from some shading effects due to the proximity to the release pipe.

The KFX™ model performance on the thermal radiation predictions for Jet Fire No. 1 is presented in Fig. 5. The left side of Fig. 5 shows another way of comparing predicted and observed incident thermal radiation at the thirteen radiometer locations. Here, the diagonal line represents predictions that match perfectly with measurements. The lower dotted line represents a predicted incident thermal radiation that is a factor of two below the measured incident thermal radiation. The upper dotted line represents predicted incident thermal radiation that is a factor of two above the measured incident thermal radiation. On the right side of Fig. 5 statistical evaluation parameters are applied to quantify the model performance against experimental data [17, 18]. The geometric mean bias (MG) and the geometric mean variance (VG) can be defined as $MG = \exp(< \ln(P/O) >)$ and $VG = \exp(< (\ln(P/O))^2 >)$, respectively, where $< >$ means averaging over all locations where values are obtained. Here, P stands for the predicted mean incident thermal radiation, and O stands for the corresponding observed mean incident thermal radiation. In Fig. 5 (right side), the geometric mean bias (MG) is plotted versus the geometric mean variance (VG) for the predicted and measured incident thermal radiation from Jet Fire No. 1 (including all thirteen radiometers). When the geometric mean is plotted versus the geometric mean variance, the model performance can be evaluated based on comparison with a parabola curve. Points at MG=VG=1 indicate that the predicted incident thermal radiation is exactly equal to the observed incident thermal radiation. Points occurring to the left of the vertical line at MG=1 indicate that observed incident thermal radiation is underpredicted, and points occurring to the right of MG=1 indicate that observed incident thermal radiation is overpredicted. Points on the parabola curve indicate that the model under- or overpredicts the observed incident thermal radiation consistently with the same factor for all predictions. The two vertical dotted lines represent predictions that are a factor of two below or above the observed incident thermal radiation.

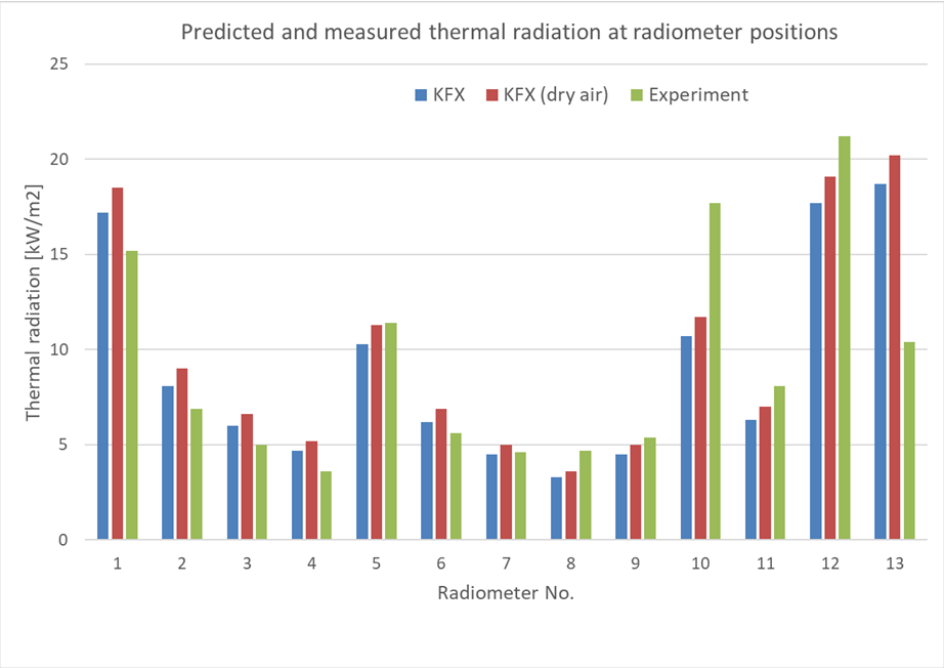

Figure 4. Comparison of predicted and measured thermal radiation at different radiometer locations for Jet Fire No. 1.

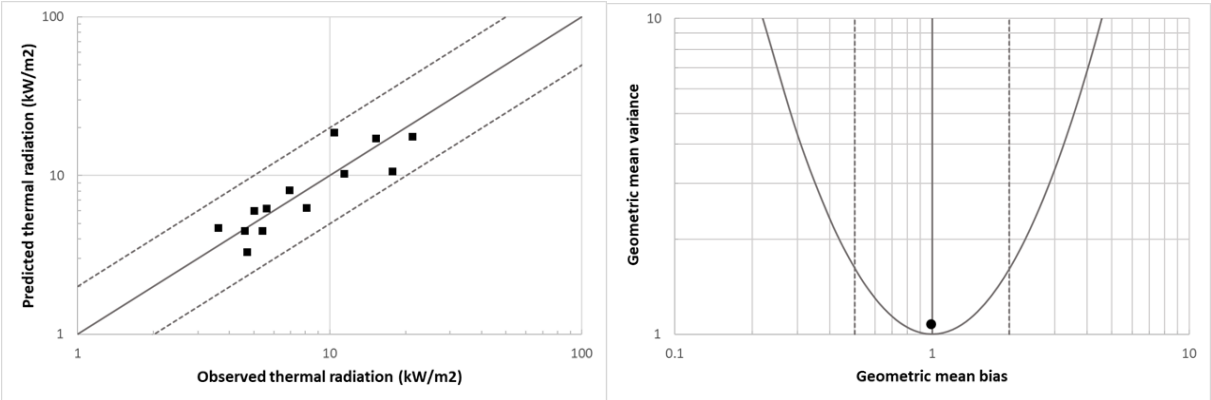

Figure 5. KFX™ model performance for Jet Fire No. 1.

For Jet Fire No. 1 in total, the incident thermal radiation is underpredicted by a factor of 0.987. The fraction of energy released as thermal radiation was predicted by KFX™ to be 14.7 % for this hydrogen jet fire. For the same hydrogen jet fire, Ekoto et al. [6] reported the average radiant fraction found in the experiment to be 21 % (excluding Radiometer No. 6, 7, 8 and 13) and calculated the average radiant fraction (based on four different pseudo-source models) to be between 13 % and 15 %. On the other hand, Advantica estimated the radiant fraction for the same jet fire to be approximately 12 % when they performed the experiments [19].

Figure 6 shows predicted iso-contours of projected maximum gas temperature for Jet Fire No. 2. In the jet fire experiment, significant visible flame luminosity was observed with bright yellow and orange colours that is typically not observed for smaller hydrogen flames. This is a result of saturated emission lined in the visible part of the electromagnetic spectrum. In the experiment, the flame length was estimated to be 48.5 m [6]. The predicted iso-contours of projected maximum gas temperature in Fig. 6 indicate a predicted flame that is some shorter than the estimated flame length from the experiment. Figure 7 shows a detailed comparison of the predicted incident thermal radiation to the measured incident thermal radiation at the thirteen radiometer locations. Simulation results for

atmospheric conditions with dry air are also included for comparison for Jet Fire No. 2. As expected, the predicted incident thermal radiation is a little higher for atmospheric conditions with dry air than for atmospheric conditions with humid air. The overall agreement between the predicted and measured incident thermal radiation is very good. Some deviations between predictions and measurements are especially observed for radiometer No. 8 and radiometer No.13 for Jet Fire No. 2. Radiometer No. 8 is positioned directly downstream of the flame, orientated along the release axis. The lower predicted incident thermal radiation for this radiometer may be explained by a shorter predicted jet flame compared to the jet flame in the experiment. Possible reasons for the deviation between the predicted and measured incident thermal radiation at radiometer No. 13 for Jet Fire No. 2 will be similar to what was discussed for the same radiometer for Jet Fire No. 1, as the radiometer was located at the same position in both experiments. Figure 8 presents the KFX™ model performance on the thermal radiation predictions for Jet Fire No. 2. The left side of Fig. 8 shows a comparison of predicted and observed incident thermal radiation at the thirteen radiometer locations. On the right side of Fig. 8, the geometric mean bias (MG) is plotted versus the geometric mean variance (VG) for the predicted and measured incident thermal radiation from Jet Fire No. 2 (including all thirteen radiometers). For Jet Fire No. 2 in total, the incident thermal radiation is underpredicted by a factor of 0.912. The fraction of energy released as thermal radiation was predicted by KFX™ to be 17.6 % for this hydrogen jet fire. For Jet Fire No. 2, Ekoto et al. [6] reported the average radiant fraction found in the experiment to be 29 % (excluding Radiometer No. 6, 7, 8 and 13) and calculated the average radiant fraction (based on four different pseudo-source models) to be between 15 % and 17 %. When Advantica performed this jet fire experiment, they estimated the radiant fraction to be approximately 19 % [19].

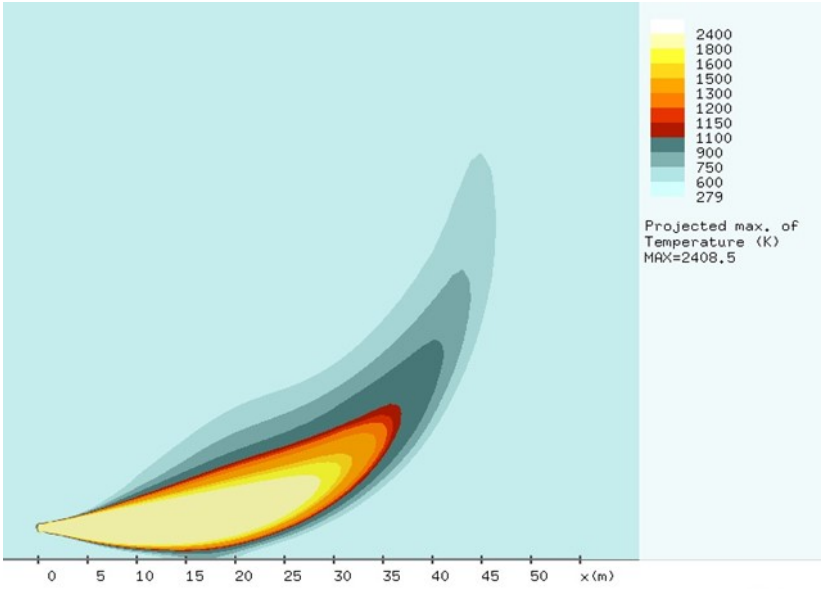

Figure 6. Predicted iso-contours of projected maximum gas temperature for Jet Fire No. 2.

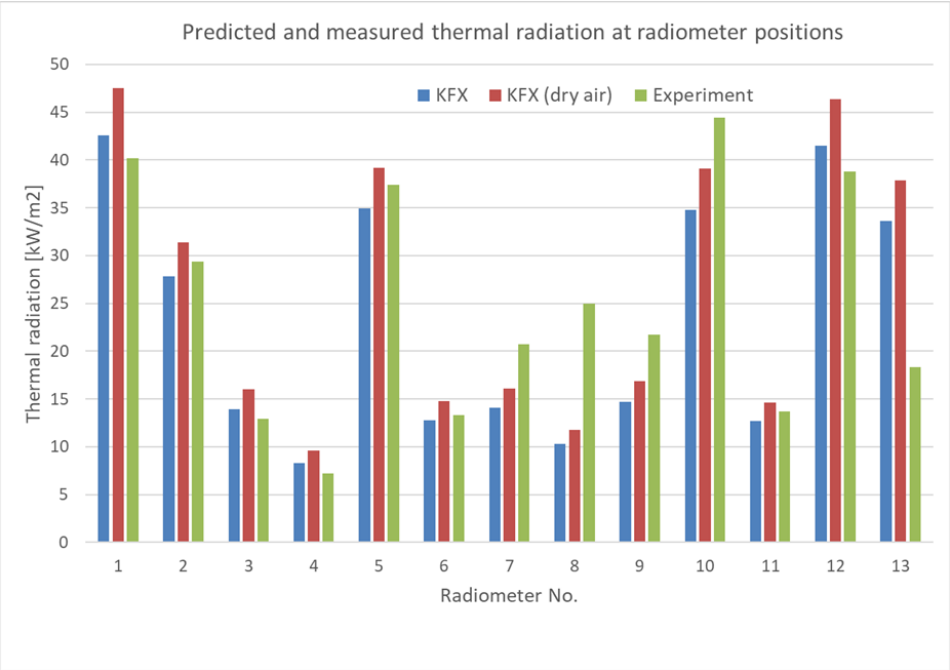

Figure 7. Comparison of predicted and measured thermal radiation at different radiometer locations for Jet Fire No. 2.

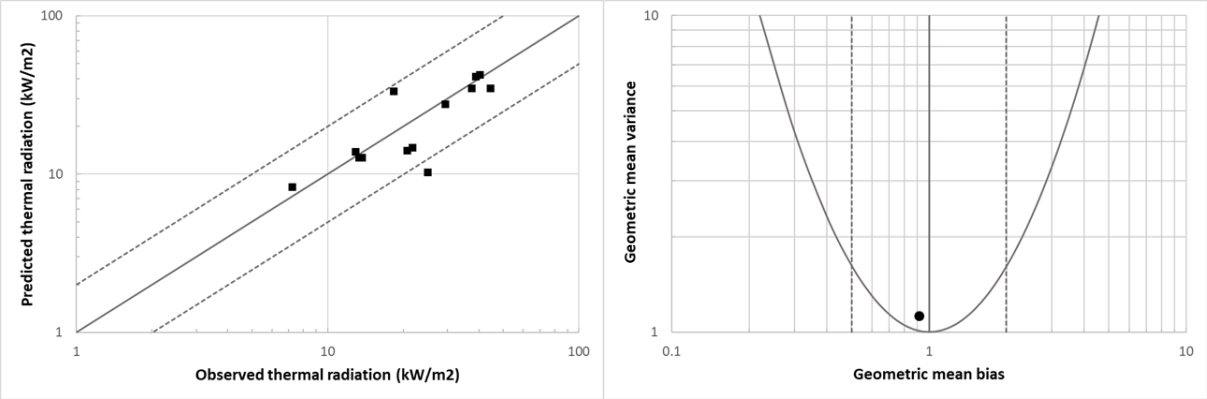

Figure 8. KFX™ model performance for Jet Fire No. 2.

For both jet fire experiments, the accuracy of the radiometers was reported to be ±5 % [6], but flame temperatures were not measured. A more detailed comparison of flame characteristics is therefore difficult from the available experimental information. Additional simulations were performed for Jet Fire No. 1 to check the KFX™ model sensitivity of ground surface reflectance on the predicted incident thermal radiation at the radiometer locations. Here, only a relatively minor effect of different values of ground surface reflectance was observed. Furthermore, grid sensitivity was tested for the simulation of Jet Fire No. 1, where the present results were compared to results from a fine-grid KFX™ simulation with 2949160 computational cells. No significant differences were observed between these simulation results.

7.0 CONCLUSION

Two large-scale hydrogen jet fires (1.0 kg H_2/s and 7.5 kg H_2/s, respectively) have been simulated with the industrial CFD code KAMELEON FIREEX KFX®. For the present simulations, the high-pressure hydrogen gas release source is modelled using a pseudo-source concept based on accurate real-gas thermodynamic data for hydrogen. The turbulent hydrogen-air combustion is modelled using

the Eddy Dissipation Concept by Magnussen, and thermal radiation calculations are based on the discrete transport method of Lockwood and Shah. Radiative properties of water vapour are modelled according to Leckner. Overall, the predicted incident thermal radiation by KFX™ is found to be in very good agreement with the measured incident thermal radiation for the simulated large-scale hydrogen jet fires, especially when considering the complexity and variability of such large-scale experiments. The results demonstrate that KFX™ can be applied as a predictive tool for industrial hazard analysis of such hydrogen jet fires. Further model validation against data from large-scale hydrogen fire experiments is recommended to investigate model performance for other scenarios, such as large-scale hydrogen jet fires in realistic, complex geometries.

ACKNOWLEDGMENTS

The author gratefully acknowledges the financial support from the Research Council of Norway for BIA project No. 261752.

REFERENCES

1. Lowesmith, B.J., Hankinson, G., Acton, M.R. and Chamberlain, G., An Overview of the Nature of Hydrocarbon Jet Fire Hazards in the Oil and Gas Industry and a Simplified Approach to Assessing the Hazards, *Trans. IChemE, Part B, Process Safety and Environmental Protection*, **85** (B3), 2007, pp. 207-220.
2. Hankinson, G. and Lowesmith, B.J., A Consideration of Methods of Determining the Radiative Characteristics of Jet Fires, *Combustion and Flame*, **159**, 2012, pp. 1165-1177.
3. Schefer, R.W., Houf, W.G., Bourne, B. and Colton, J., Spatial and Radiative Properties of an Open-Flame Hydrogen Plume, *International Journal of Hydrogen Energy,* **31**, 2006, pp. 1332-1340.
4. Schefer, R.W., Houf, W.G., Williams, T.C., Bourne, B. and Colton, J., Characterization of High-Pressure, Underexpanded Hydrogen-Jet Flames, *International Journal of Hydrogen Energy,* **32**, 2007, pp. 2081-2093.
5. Molina, A., Schefer, R.W. and Houf, W.G., Radiative Fraction and Optical Thickness in Large-Scale Hydrogen-Jet Fires, *Proceedings of the Combustion Institute*, **31**, 2007, pp. 2565-2572.
6. Ekoto, I.W., Houf, W.G., Ruggles, A.J., Creitz, L.W. and Li, J.X., Large-Scale Hydrogen Jet Flame Radiant Fraction Measurements and Modeling, Proceedings of the 2012 9th International Pipeline Conference (IPC2012), 24-28 September 2012, Calgary, Alberta, Canada.
7. Magnussen, B.F., Rian, K.E., Grimsmo, B., Lilleheie, N.I., Kleiveland, R.N. and Vembe, B.E., Computational Analysis of Large-Scale Fires in Complex Geometries – a Means to Safeguard People and Structural Integrity in the Oil and Gas Industry, *Chemical Engineering Transactions*, **31**, 2013.
8. Magnussen, B.F., The Eddy Dissipation Concept – a Bridge between Science and Technology, Invited paper at ECCOMAS Thematic Conference on Computational Combustion, 21-24 June 2005, Lisbon, Portugal.
9. Magnussen, B.F., On the Structure of Turbulence and a Generalised Eddy Dissipation Concept for Chemical Reactions in Turbulent Flow, 19th AIAA Aerospace Science Meeting, 12-15 January 1981, St. Louis, Missouri, USA.
10. Shah, N.G., The Computation of Radiant Heat Transfer, Ph.D. Thesis, University of London, Faculty of Engineering, UK, 1979.
11. Leckner, B., Spectral and Total Emissivity of Water Vapor and Carbon Dioxide, *Combustion and Flame*, **19**, 1972, pp. 33-48.
12. Rian, K.E., Simplified modelling and calculation of high-pressure gas jets. SINTEF Report No. STF84 F97515, 1997.
13. Vembe, B.E., Rian, K.E., Holen, J.K., Lilleheie, N.I., Grimsmo, B. and Myhrvold, T., Kameleon FireEx 2000 Theory Manual, ComputIT Report No. R0123, 2001.

14. Leachman, J.W., Jacobsen, R.T., Penoncello, S.G. and Lemmon, E.W., Fundamental Equations of State for Parahydrogen, Normal Hydrogen, and Orthohydrogen, *J. Phys. Chem. Ref. Data*, **38** (3), 2009.
15. NIST Standard Reference Database 69: *NIST Chemistry WebBook*, visited January 2017, National Insitute of Standards and Technology, U.S. Department of Commerce.
16. Vembe, B.E., Kleiveland, R.N., Grimsmo, B., Lilleheie, N.I., Rian, K.E., Olsen, R., Lakså, B., Nilsen, V., Vembe, J.E. and Evanger, T., KFX™ User Manual, ComputIT Report No. R1706, 2017.
17. Hanna, S.R., Chang, J.C. and Strimaitis, D.G., Hazardous Gas Model Evaluation with Field Observations, *Atmospheric Environment*, **27A** (15), 1993, pp. 2265-2285.
18. Commission of the European Communities, Gas Explosion Model Evaluation Protocol, Model Evaluation Group for Gas Explosions, 1997.
19. Allason, D., Personal Communication, June 2018.